The EMBO Journal vol.8 no.8 pp.2179–2188, 1989

High-resolution X-ray diffraction study of the complex between endothiapepsin and an oligopeptide inhibitor: the analysis of the inhibitor binding and description of the rigid body shift in the enzyme

A.Šali[1,3], B.Veerapandian[1], J.B.Cooper[1], S.I.Foundling[1,4], D.J.Hoover[2] and T.L.Blundell[1]

[1]Laboratory of Molecular Biology, Department of Crystallography, Birkbeck College, University of London, London WC1E 7HX, UK, and [2]Department of Medicinal Chemistry, Pfizer Central Research, Groton, CT 06340, USA

[3]On leave from: Department of Biochemistry, J.Stefan Institute, Ljubljana, Yugoslavia
[4]Current address: E.I.Du Pont De Nemours & Co. Inc., Central Research & Development, Wilmington, DE 19880, USA

Communicated by T.L.Blundell

The conformation of the synthetic renin inhibitor CP-69,799, bound to the active site of the fungal aspartic proteinase endothiapepsin (EC 3.4.23.6), has been determined by X-ray diffraction at 1.8 Å resolution and refined to the crystallographic *R* factor of 16%. CP-69,799 is an oligopeptide transition–state analogue inhibitor that contains a new dipeptide isostere at the P_1-P_1' position. This dipeptide isostere is a nitrogen analogue of the well-explored hydroxyethylene dipeptide isostere, wherein the tetrahedral P_1' C_α atom has been replaced by trigonal nitrogen. The inhibitor binds in the extended conformation, filling S_4 to S_3' pockets, with hydroxyl group of the P_1 residue positioned symmetrically between the two catalytic aspartates of the enzyme. Interactions between the inhibitor and the enzyme include 12 hydrogen bonds and extensive van der Waals contacts in all the pockets, except for S_3'. The crystal structure reveals a bifurcated orientation of the P_2 histidine side chain and an interesting relative rotation of the P_3 phenyl ring to accommodate the cyclohexyl side chain at P_1. The binding of the inhibitor to the enzyme, while producing no large distortions in the enzyme active site cleft, results in small but significant change in the relative orientation of the two endothiapepsin domains. This structural change may represent the action effected by the proteinase as it distorts its substrate towards the transition state for proteolytic cleavage.

Key words: X-ray/endothiapepsin/oligopeptide inhibitor/aspartic proteinases/conformational changes

Introduction

The family of aspartic proteinases is characterized by two aspartates essential for catalytic activity (Chen and Tang, 1972; Hartsuck and Tang, 1972) and by specific inhibition by microbial antibiotic pepstatin (Umezawa *et al.*, 1970). X-ray crystallography has provided three-dimensional structures of several members of the family, including porcine pepsin (Andreeva *et al.*, 1984), human renin (Sielecki *et al.*, 1989) and the zymogen of pepsin, pepsinogen (James and Sielecki, 1986). In addition, the structures of three fungal enzymes, penicillopepsin (James and Sielecki, 1983), rhizopuspepsin (Bott *et al.*, 1982; Suguna *et al.*, 1987a) and endothiapepsin (Pearl and Blundell, 1984; Blundell *et al.*, 1985) from *Penicillium janthinellum, Rhizopus chinensis* and *Endothia parasitica*, respectively, are known. These structures reveal many common features. They consist of two predominantly β-sheet domains that are related by a ~2-fold axis. The bilobal architecture probably evolved by gene duplication, fusion and sequence divergence (Tang *et al.*, 1978). The extended active site groove capable of accommodating roughly eight residues (Fruton, 1976) is situated between the two domains, each providing one of the essential aspartates, Asp-32 and Asp-215 (pepsin numbering). The two aspartates reside in the middle of the cleft, at the tip of the loops containing diad related and highly conserved Asp-Thr-Gly-Ser/Thr sequences. The aspartate side chains are within hydrogen bonding distance from each other and approximately co-planar due to the constraints of a 'fireman's' grip network of hydrogen bonds that involves conserved hydroxyl functions of Thr at positions 33 and 216 (Pearl and Blundell, 1984). A solvent molecule is hydrogen bonded symmetrically to both catalytic aspartates in the native enzymes (Pearl and Blundell, 1984; James and Sielecki, 1985; Suguna *et al.*, 1987b) and it may play the role of a nucleophile in catalysis.

Clinically, the most interesting aspartic proteinase is human kidney renin. The only known function of renin is the cleavage of decapeptide angiotensin I from the N-terminus of angiotensinogen. This is the first and rate limiting step in the conversion of angiotensinogen into the octapeptide angiotensin II, a potent vasoconstrictor and effector of aldosterone secretion. Inhibitors of the angiotensin converting enzyme (ACE), a carboxypeptidase catalysing the second step of angiotensin conversion, are already commercially available as antihypertensive drugs (Ondetti and Cushman, 1980). Therefore, specific human renin inhibitors are also expected to be effective in lowering blood pressure. Many substrate analogues, with K_i values approaching the micromolar range, have been synthesized (Haber and Burton, 1979; Haber, 1984). However, only the replacement of the scissile bond with various surrogates of the postulated tetrahedral transition-state has yielded transition-state analogue inhibitors with K_i values in the nanomolar range (Szelke *et al.*, 1982; Hofbauer and Wood, 1985).

X-ray crystallographic studies of the co-crystallized complexes of rhizopuspepsin and penicillopepsin with pepstatin and a pepstatin fragment provided the first information on the binding of transition state inhibitors to aspartic proteinases (Bott *et al.*, 1982; James *et al.*, 1982; Bott and Davies, 1983). Modelling of human renin, based on the homology with other aspartic proteinases, has shown that renin may assume a similar structure (Blundell *et al.*, 1983; Sibanda *et al.*, 1984; Akahane *et al.*, 1985; Carlson *et al.*, 1985; Hemmings *et al.*, 1985). This encouraged us

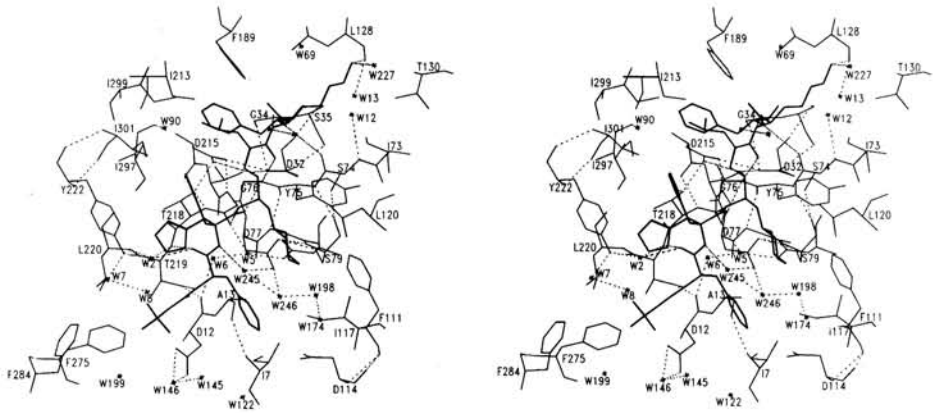

Fig. 1. The binding of CP-69,799 to the active site cleft of endothiapepsin. Stereo view of the complex between endothiapepsin (thin line) and CP-69,799 (thick line) showing the hydrogen bonds (dotted lines) and the extensive van der Waals contacts between the inhibitor and the enzyme. Only the enzyme residues that are less than 5 Å from the inhibitor are included.

to co-crystallize and study several transition-state analogue inhibitors with endothiapepsin (Hallett *et al.*, 1985; Foundling *et al.*, 1987; Cooper *et al.*, 1987a,b, 1988; Blundell *et al.*, 1987). The similarity of the overall fold of renin and that of other aspartic proteinases has recently been confirmed by X-ray analysis of human renin (Sielecki *et al.*, 1989).

We report here the structure of the complex between the inhibitor CP-69,799 and endothiapepsin. CP-69,799 (Hoover *et al.*, in preparation) is an inhibitor of human plasma renin ($IC_{50} = 3 \times 10^{-7}$ M) *in vitro* and is a potent inhibitor of hog renin both *in vitro* ($IC_{50} = 10^{-9}$ M) and *in vivo* (Hoover *et al.*, in preparation). It contains a new scissile bond surrogate, wherein the (*S*)-hydroxyethylene moiety replaces the peptide function and a nitrogen atom replaces the P_1' C_α atom. This azahomostatine (AHS) dipeptide isostere corresponds formally to the hydroxyethylene dipeptide (homostatine) isostere, except that the P_1' substituent is disposed from trigonal nitrogen rather than from tetrahedral carbon; the inhibitor is thus a trisubstituted urea with conformational and hydrogen bonding constraints different from previously studied inhibitors. Additionally, CP-69,799 has a polar lysine residue at the P_2' position in contrast with the lipopholic residues of these compounds.

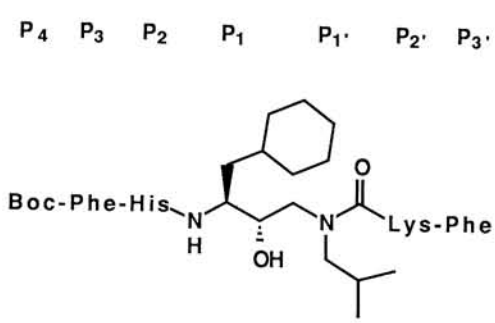

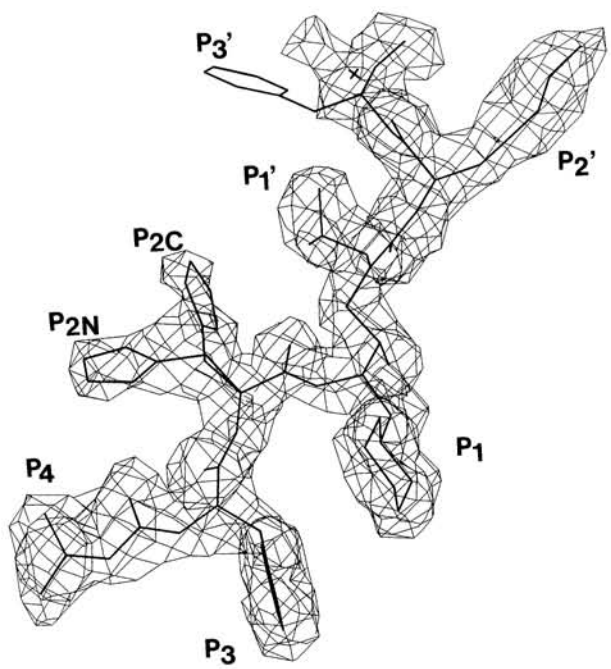

Fig. 2. The final electron density map calculated with the $2|F_o| - |F_c|$ coefficients for the CP-69,799 inhibitor in the active site cleft of endothiapepsin. The complex was refined at 1.8 Å to an *R* factor of 16%. The final electron density map for the inhibitor defines all positions, except C-terminal P_3' Phe. For the comments on bifurcated His at P_2 see Results and discussion.

Results and discussion

Overall view

The oligopeptide inhibitor, which adopts an extended conformation, fits well in the long active site cleft of endothiapepsin, with the 'flap' region covering the inhibitor and completely shielding it from the solvent in the central P_1-P_1' region (Figure 1). The carboxyl terminal P_3' Phe, which loops out of the 'flap', and P_4 Boc at the N-terminus are exposed to the solvent. The hydroxyl group at the P_1 position is located symmetrically between the catalytic aspartates 32 and 215. The water molecule bound to these two residues in the native enzyme is displaced in the complex. The inhibitor makes several hydrogen bonding, van der Waals and possibly ionic interactions with both the first and second domain of the enzyme.

Electron density

Figure 2 shows the final map calculated with weighted $2|F_o| - |F_c|$ coefficients (Read, 1986) for the inhibitor. The map is continuous from Boc [tert-butyloxycarbonyl] at

Table I. Main chain and side chain dihedral angles of CP-69,799[a]

Position and residue		Angle (degrees)						
		Φ	Ψ	ω	χ_1	χ_2	χ_3	χ_4
P_3	Phe	−87	152	179	−77 g^+	−49		
P_{2N}	His	−140	90	−168	−44 g^+	64		
P_{2C}	His	−139	93	−168	−168 t	22		
P_1	AHS[b]	−111	45	153	−69 g^+	−50		
P_1'	AHS[b]	−77	171	171	73 g^-	82		
P_2'	Lys	−90	127	−178	−165 t	−155	159	−178
P_3'	Phe	−139			−125 g^+	−141		

[a]The rotamer conformations for χ_1 angle, using the nomenclature of Janin *et al.* (1978), are also shown.
[b]Note that AHS is a dipeptide analogue that does not have a peptide bond. In addition, the leucyl side chain at P_1' does not branch from the tetrahedral C_α atom but from the planar nitrogen atom.

P_4 to Lys at P_2' position. The only residue whose position is not seen is the carboxyl-terminal P_3' Phe. There is a bifurcated density for the P_2 His side chain. The two orientations, P_{2C} His and P_{2N} His, are the t and g^+ conformations respectively. The notation for describing side chain rotamers introduced by Janin *et al.* (1987) will be used throughout this paper.

Conformation

Main chain and side chain dihedral angles for the inhibitor are shown in Table I. All main chain dihedral angles are in the β-sheet area of the Ramachandran plot. It is interesting that the ω dihedral angle of −168° for P_2 His is significantly different from its ideal value of 180° (Figure 3); the standard deviation of the 329 ω dihedral angles of endothiapepsin is 0.7°. The unfavourable energy change associated with the ω dihedral angle of −168° can be estimated to be 5−10 kJ/mol (Shipman and Christoffersen, 1972). All five refined endothiapepsin inhibitor complexes which have His at P_2 (H142, H261, L-363,564, H77 and H189) also acquired distorted P_2 ω dihedral angles. The mean value for these five inhibitors is −168° with a standard deviation of 4°. It must be noted, however, that H256, with glutamyl side chain at P_2, and the reduced peptide inhibitor in rhizopuspepsin complex, with P_2 His (Suguna *et al.*, 1987b), have a normal ω angle of ~180°. The following interactions between the inhibitor and the enzyme may contribute to the stabilization of the P_2-P_1 peptide bond distortion in the inhibitor complex. First, the geometry of the bifurcated hydrogen bond from O of P_2 to 'flap' amide nitrogens of Gly-76 and Asp-77 is improved by the observed twist in the P_2-P_1 peptide bond (Figure 3). Second, the main chain at both ends of the P_2-P_1 peptide bond is fastened in place by the main chain hydrogen bonds and interactions between the inhibitor side chains and the enzyme pockets. Since there is no dependence on the type of the scissile bond surrogate, a general strain mechanism as suggested by Pearl and Blundell (1984) may exist. The role in proteolysis of the strain at P_2-P_1 peptide bond, as opposed to P_1-P_1' peptide bond, is not clear. However, the observed tilt of the P_2 carbonyl would improve the geometry of the hydrogen bond to the tetrahedral P_1' nitrogen in the hypothetical transition-state (Suguna *et al.*, 1987b), thereby stabilizing the transition-state and hence improving catalytic efficiency of the enzyme.

If the observed side chain dihedral angles (Table I) are compared with the corresponding dihedral angles in the rotamer library of Ponder and Richards (1987), one finds that the distribution is similar to that found in proteins in general. The P_2' Lys side chain is in the second most populated t conformation. It is extended and very well defined in the electron density. This can be correlated with two hydrogen bonds from the terminal side chain nitrogen, one to carbonyl oxygen of Leu-128, another to water molecule W227 which is further hydrogen bonded to the enzyme. The P_1 cyclohexyl side chain also adopts a very favourable g^+ conformation, minimizing intra-chain non-bonded interactions. The cyclohexyl ring is in its most stable chair conformation.

The Boc group at P_4 position is in a planar *anti* conformation. Five atoms of the Boc group (CB1, CA, OB, C and O) and two atoms of the P_3 phenyl (N and CA) are all within 0.03 Å from their least squares plane.

The P_1-P_1' ω dihedral angle of 153° in CP-69,799 may reflect the corresponding change in the hybridization of the planar P_1' nitrogen of the substrate as it proceeds to the tetrahedral intermediate during the hydrolysis catalysed by the enzyme.

Water molecules

The inhibitor displaces 23 water molecules, including the water molecule originally located between the two catalytic aspartates. All 11 enzyme groups that are involved in the inhibitor hydrogen bonding are also hydrogen bonded to water molecules in the native enzyme (according to 3.5 Å cut-off for the donor−acceptor distance). Out of 16 water molecules which are closer than 4.2 Å to the inhibitor in the complex, only seven have approximately equivalent positions in the free enzyme crystal (W5, W6, W12, W13, W145, W174 and W246). All of these conserved waters are either extensively hydrogen bonded or are in the deep pockets formed by the enzyme matrix (Figure 1).

Hydrogen bonds

The inhibitor forms 12 hydrogen bonds to the enzyme and three to water molecules (Figure 4). In the N-terminal part of the inhibitor, Thr-219 participates in two hydrogen bonds to P_3 residue: the side chain oxygen of Thr-219 is hydrogen bonded to the amide nitrogen of P_3 and the amide nitrogen of Thr-219 interacts with the carbonyl oxygen of the P_3 Phe. The carbonyl oxygen of the P_3 Phe is also hydrogen bonded to the water molecule W2. The P_2 imidazole, but only in P_{2C} conformation, is hydrogen bonded to the side chain oxygen of the Thr-218.

In the central and C-terminal part of the inhibitor there are four hydrogen bonds to the 'flap' residues: (1) the amide nitrogen of Asp-77 is hydrogen bonded to the carbonyl oxygen of P_2, (2) this carbonyl oxygen of P_2 is also involved in a rather weak hydrogen bond interaction with the amide nitrogen of Gly-76, (3) the same amide nitrogen participates in the third 'flap' hydrogen bond to the carbonyl oxygen of the P_1 urea unit and (4) the carbonyl oxygen of Ser-74 is hydrogen bonded to the amide nitrogen of P_3'. In addition, the amide nitrogens of P_1 and P_2' are hydrogen bonded to the carbonyl oxygens of Gly-217 and Gly-34, respectively. The hydroxyl group of the azahomostatine presumably makes two hydrogen bonds at the pH of the analysis (pH 4.5), most likely to the side chain oxygens OD1 of the aspartates 32 and 215. There are also two hydrogen bonds from the P_2' Lys side chain mentioned above. The only other inhibitor complex with a P_2' side chain capable

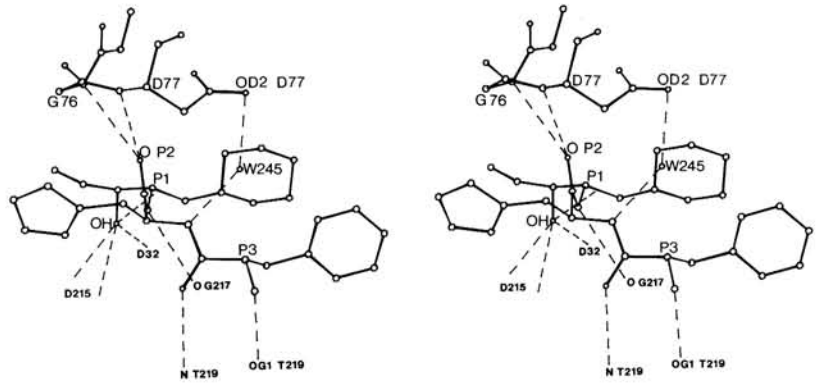

Fig. 3. The distortion of the inhibitor ω dihedral angle at P_2. The inhibitor main chain is viewed from the N- to C-terminus. The geometry of the bifurcated 'flap' hydrogen bond from the O of P_2 to N of Gly-76 and N of Asp-77 is improved by distorting the P_2-P_1 peptide bond to the ω angle of 168°. This distortion is also facilitated by the tight binding of the inhibitor main chain before and after the P_2-P_1 peptide bond. Note that the main chain is engaged in several hydrogen bonds and, via side chains, also in many van der Walls contacts. The P_2-P_1 peptide bond distortion may have a role in a catalytic mechanism by improving the geometry of a postulated hydrogen bond between the titled O of P_2 and tetrahedral nitrogen at P_1 of the transition state (Suguna *et al.*, 1987b).

of hydrogen bonding is that of H256 with the P_2' arginine. This arginine side chain hydrogen bonds similarly to a water molecule and the carbonyl oxygen of Leu-128 (Cooper *et al.*, 1987b).

The hydrogen bond between the main chain nitrogen of P_2 and water W245 has not been observed before. Water W245 is further hydrogen bonded to the side chain oxygen of the Asp-77 side chain (Figures 1 and 3). However, an alternative interpretation of the $2|F_o| - |F_c|$ and $|F_o| - |F_c|$ maps is possible, where the position of the water W245 is occupied by the other side chain oxygen of the Asp-77. The first possibility is adopted here, mainly because this arrangement undoubtedly occurs in the H261 complex (refined at 1.6 Å to $R = 0.14$; B.Veerapandian, J.B.Cooper, M.Szelke and T.L.Blundell, in preparation). In contrast, a reduced peptide inhibitor bound to rhizopuspepsin (Suguna *et al.*, 1987b), a pepstatin inhibitor bound to penicillopepsin (James and Sielecki, 1985) and an H189 statine inhibitor bound to endothiapepsin (D.Bailey, J.B.Cooper, B.Veerapandian and T.L.Blundell, in preparation) form a hydrogen bond directly between the main chain nitrogen of P_2 residue and the oxygen of the Asp-77 side chain (endothiapepsin numbering) with no water molecule in between.

The comparison of hydrogen bonds between endothiapepsin and various inhibitors (H142, H256, L-363,564, ACRIP, H261, H77, BW624, H189 and CP-69,799) reveals an almost absolute conservation of hydrogen bonds between the inhibitor main chain and the enzyme (Figure 4). In contrast, the inhibitor to water hydrogen bonds and inhibitor side chain to enzyme hydrogen bonds vary a great deal. The differences in side chains and water hydrogen bonding are not correlated with the inhibitor potency (Foundling *et al.*, 1987). These data are consistent with the view that only the main chain hydrogen bonding to the enzyme, not the inhibitor side chain hydrogen bonding and hydrogen bonding to water molecules, is important for the inhibition.

In order to interpret the role of the ligand main chain hydrogen bonding, one has to examine the changes that occur during formation of hydrogen bonds. Before the complex is formed, the hydrogen bonding donors and acceptors are already hydrogen bonded to water molecules (see also 'Water molecules'). Therefore, the free energy contribution of the

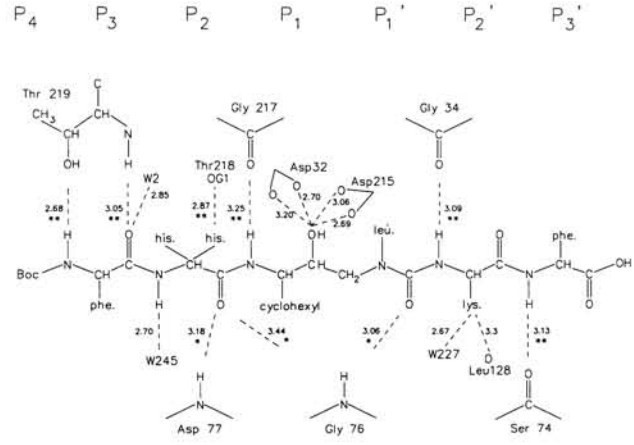

Fig. 4. Hydrogen bonds between the CP-69,799 inhibitor and its environment. Hydrogen bonds of the inhibitor main chain and side chains to the enzyme and water molecules are shown schematically. The distances between hydrogen bond acceptors and donors are specified in Ångstroms. The side chain nitrogen ND1 of the P_{2C} His is hydrogen bonded to the side chain oxygen of Thr-218. Note the antiparallel β-sheet pattern of hydrogen bonds involving inhibitor main chain and enzyme residues Ser-76, Asp-77 and, on the other side, Gly-217 and Thr-219. Only two inhibitor side chains are hydrogen bonded to the enzyme (His P_{2C} to the side chain oxygen of Thr-218 and Lys P_2' to the carbonyl oxygen of Leu-128) and only three water molecules are hydrogen bonded to the inhibitor (W2 to the carbonyl oxygen P_3, W245 to the amide nitrogen of P_2 and W227 to the side chain nitrogen of Lys P_2'). The hydrogen bonds that are observed in all endothiapepsin complexes with the positions P_3-P_3' occupied are indicated by two stars and the hydrogen bonds that are usually observed are indicated by one star.

hydrogen bonds between the enzyme and ligand to the binding reaction is expected to be small, if any at all, especially since some of these hydrogen bonds are distorted and no charged groups are involved (Fersht *et al.*, 1986) (Figure 4). Accordingly, the conserved ligand main chain hydrogen bonds are probably crucial only for the precise alignment of the ligand in the enzyme active site cleft, whereas the binding potency must be contributed by other interactions, most probably van der Waals contacts between ligand side chains and the enzyme binding pockets. In contrast to the hydrogen bonds, the free energy change for

Table II. Enzyme binding pockets for the CP-69,799 complex[a]

Position	P_4 Boc	P_3 Phe	P_{2N} His	P_{2C} His	P_1 AHS	P_1' AHS	P_2' Lys	P_3' Phe
	12 Asp	7 Ile	75 Tyr	75 Tyr	30 Asp	34 Gly	34 Gly	74 Ser
	219 Thr	12 Asp	76 Gly	76 Gly	32 Asp	35 Ser	73 Ile	76 Gly
	220 Leu	13 Ala	77 Asp	77 Asp	75 Tyr	75 Tyr	74 Ser	297 Ile
	222 Tyr	114 Asp	117 Ile	217 Gly	77 Tyr	76 Gly	128 Leu	299 Ile
	275 Phe	117 Ile	217 Gly	218 Thr	79 Ser	189 Phe	130 Thr	12 W
	284 Phe	217 Gly	218 Thr	297 Ile	111 Phe	213 Ile	189 Phe	14 W
	2 W	218 Thr	222 Tyr	301 Ile	120 Leu	215 Asp	12 W	90 W
	7 W	219 Thr	297 Ile	244 W	215 Asp	299 Ile	13 W	
	8 W	2 W	8 W		217 Gly		69 W	
	145 W	5 W	245 W		218 Thr		227 W	
	245 W	6 W			5 W			
		245 W			174 W			
		246 W			198 W			
					245W			
					246W			
Electron density	Good	Medium	Medium	Medium	Good	Good	Good	Weak
Number of hydrogen bonds (enzyme:water)	0:0	2:1	2:1	3:1	3:0	1:0	2:1	1:0
Number of contacts	16	43	35	39	51	29	25	20
Number of enzyme C atoms	2	12	12	14	12	13	4	3
Number of enzyme O and N atoms	8	23	8	6	14	3	7	8
Accessibility in solution (Å^2)	57.2	60.3	52.6	76.2	62.5	36.5	60.5	77.6
Accessibility in complex (Å^2)	27.1	14.4	13.6	5.6	0.9	0.8	17.9	44.5

[a]Binding pockets were defined according to the distance and accessibility criteria (see Results and discussion for definitions). The quality of the final electron density map is described. Hydrogen bonds taken into account are those from Figure 4. In *X:Y*, *X* is the number of hydrogen bonds to the enzyme and *Y* is the number of hydrogen bonds to water molecules. The number of contacts between the inhibitor atoms and surrounding enzyme atoms is shown for every inhibitor position. A cut-off distance of 4.2 Å was used. In addition, the numbers of C, N and O atoms constituting the enzyme pockets are listed for every enzyme subsite. Solvent contact areas were calculated applying the method of Richmond and Richards (1978). Solvent radius used was 1.4 Å. It was assumed that the average inhibitor conformation in solution is the same as its conformation in the complex. The accessibilities for the inhibitor positions are averages of two calculations, one with only P_{2C} and another with only P_{2N} His side chain. The areas for the bifurcated P_2 position were obtained by omitting the alternative P_2 side chain orientation.

a transfer of non-polar groups from water to non-polar enzyme environment clearly favours the complexed state.

Binding pockets

Enzyme residues that constitute the pockets of the endothiapepsin–CP-69,799 complex were defined as the union of the pocket residues obtained by two independent procedures (Table II). First, every enzyme residue which has an atom within a 4.2 Å shell centred at any inhibitor atom forms the pocket for the inhibitor residue supplying the central atom. Second, every enzyme residue which loses more than 2 Å^2 of solvent contact area upon the inhibitor binding is also part of at least one of the pockets (the conformation of endothiapepsin in the complex was used for both accessibility calculations) (Figure 5). As expected, the two procedures give almost identical results, the surface criteria identifying four more residues than the distance criteria: Ser-35 (S_1'), Ile-117 (S_3, S_1), Phe-284 (S_4) and Ile-299 (S_1', S_3'). Approximately 224 Å^2 of enzyme and 304 Å^2 of inhibitor contact area is buried upon complexation. This corresponds to 6.8 and 73% of the total enzyme and inhibitor surfaces, respectively, on the assumption that

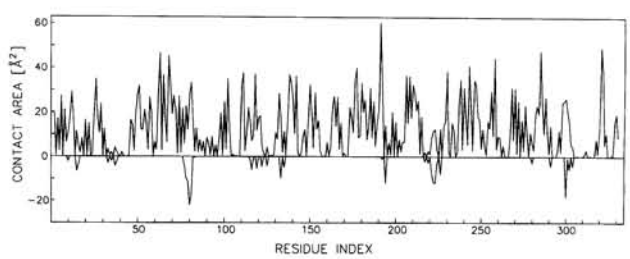

Fig. 5. Comparison of residue solvent contact areas for endothiapepsin with and without the inhibitor. The positive line is the residue contact area for the bound endothiapepsin structure without the inhibitor. The negative line is the difference between the residue contact areas for the bound enzyme structure with and without the inhibitor. Sharp peaks in the difference line allow easy identification of pocket residues. Solvent contact areas were calculated as described in the legend to Table II.

the average inhibitor conformation in solution is the same as the bound conformation. Since burying 1 Å^2 of the amino acid surface contributes ~ -0.4 kJ/mol to the free energy of the reaction (Chothia, 1974; Richmond and Richards, 1978), the hydrophobic effect contributes, by analogy, approximately -207 kJ/mol to the driving force

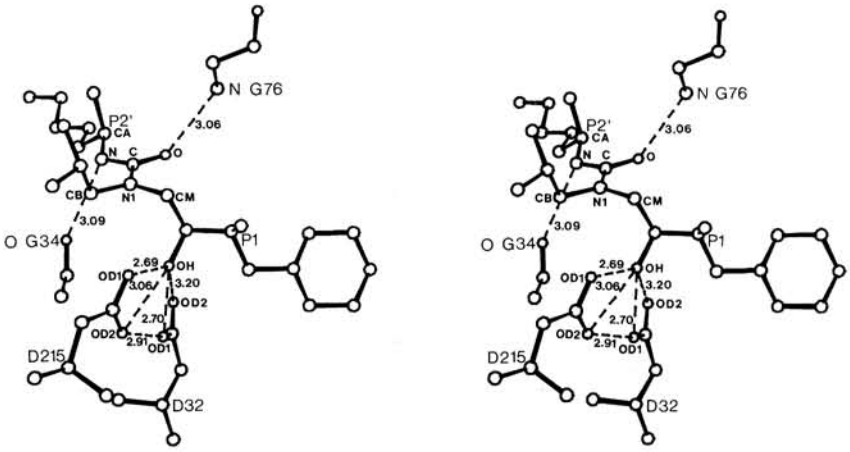

Fig. 6. The P_1 to P_2' positions of the inhibitor in the active site of endothiapepsin. The seven membered plane with the nitrogen of P_1 in the sp^2 configuration is shown together with two hydrogen bonds from the atoms of the plane to the enzyme: O P_1 to N Gly-76 and N P_2' to O Gly-34. In addition, the geometry of the constellation of the inhibitor P_1 hydroxyl and two aspartates, Asp-32 and Asp-215, is specified.

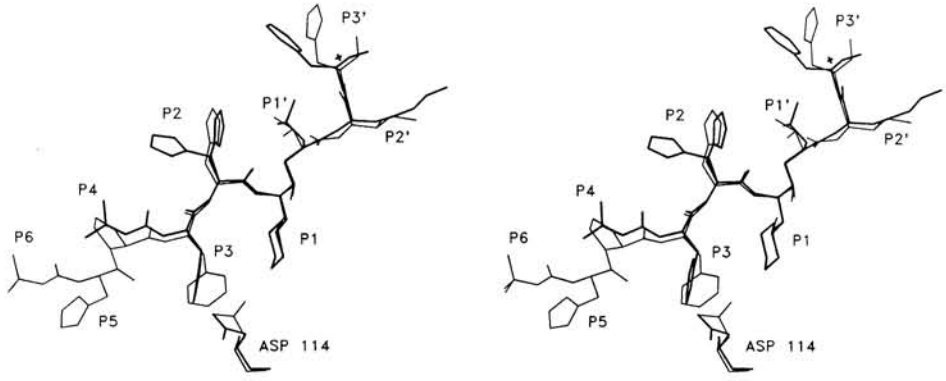

Fig. 7. Comparison of CP-69,799 and H261. The relative rotation around χ_2 of the P_3 phenyl ring gives the CP-69,799 phenyl a conformation considerably different from the more favourable one found in the H261 inhibitor (thin line; for a chemical sequence see the legend to Table III). This can be accounted for by potentially bad steric contacts between the phenyl at P_3 and the large cyclohexyl ring at P_1, if the P_3 side chain of CP-69,799 adopted the orientation found in H261. The change in the phenyl orientation is accompanied by the change in Asp-114 position. This change can be rationalized in terms of edge on packing of the phenyl ring and at least one of the Asp-114 side chain oxygens in both inhibitor complexes, an interaction shown to have a significant stabilization energy of 4–8 kJ/mol (Thomas *et al.*, 1982). The only other large change in the inhibitor conformation involves the isoleucine side chain on the planar nitrogen of urea at P_1'. It may be noted that the volume occupied by the main chain atoms is conserved, presumably because of the extensive and conserved main chain hydrogen bonding. Thus, different stereochemistry at P_1'–P_2' is reflected only in the different orientations of the P_1' isoleucine side chains.

of the inhibitor binding to the enzyme. However, the experimentally determined total standard free energy of binding at 25°C is ~ -37 kJ/mol ($\Delta G^0 = -RT\ln K_i^{-1}$; Table III). The significant difference between these two values shows that the oligopeptide inhibitor binding to aspartic proteinases, similar to protein folding, is an equilibrium process with a delicate balance determined by several large contributions, the hydrophobic effect and steric repulsions undoubtedly playing a major role.

Table II shows the extent to which the enzyme pockets restrict the access of solvent molecules to the inhibitor residues. The central inhibitor residues P_1 cyclohexyl, P_1' Leu and P_{2C} His are almost completely excluded from the solvent. At the other end of the spectrum are the terminal residues P_4 Boc and P_3' Phe with about half of their solution contact areas still accessible within the complex. P_3 Phe, P_{2N} His and P_2' Lys are slightly accessible to solvent molecules. An examination of the nature of the contacts shows that pockets P_2, P_1, P_1' and P_2' are relatively hydrophobic, whereas pockets P_4, P_3 and P_3' include a considerable proportion of polar moieties (Table II). Three convenient statistical descriptors of the enzyme pockets, i.e. number of pocket contacts between the enzyme and inhibitor, ratio of the carbon to nitrogen and oxygen atoms in a pocket and the degree of shielding of the inhibitor side chain from the solvent, are all largest for the

Table III. Kinetic constants for H261, CP-69,799 and CP-71,362

Enzyme	K_i (μM)		
	CP-69,799	CP-71,362	H261
Human renin	0.310[b]	0.020[b]	0.0007[a,b]
Endothiapepsin	0.27	0.081	<0.001[a]

[a]Hallett *et al.* (1985).
[b]Plasma IC_{50} at pH 7.0. Endothiapepsin was assayed with the substrate K-P-A-G-F-(NO_2)F-R-L at pH 3.1. CP-71,362 inhibitor is identical to the CP-69,799, except that the planar nitrogen at P_1' is replaced by a carbon atom. The chemical sequence of the H261 inhibitor is Boc-H-P-F-H-L^{h}V-I-H, where ^{h} stands for the hydroxyl scissile bond isostere.

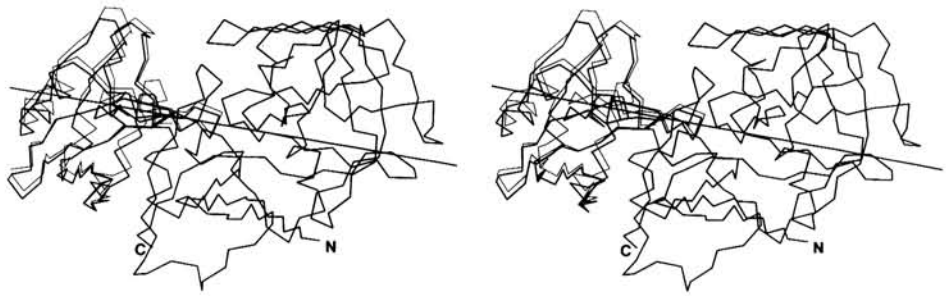

Fig. 8. Rigid body movement in endothiapepsin. This view of endothiapepsin in the CP-69,799 complex emphasizes the tripartite organization of the molecule. The rigid body consisting of residues 190–303 rotates for 4.1° around and moves for 0.3 Å along the screw axis through the residues 22 and 213. The position of the second rigid body in the native endothiapepsin is shown in thin line.

middle inhibitor positions. The inhibitor atom that contacts the greatest number of enzyme atoms is P_1 hydroxyl (11 contacts). Following are three carbonyl oxygens of P_3, P_2 and P_1' with 10, 10 and seven contacts, respectively.

The P_1-P_1' planar urea group

One of the most interesting features of the CP-69,799 inhibitor is the substitution of C_α atom of residue P_1' by a nitrogen atom. As anticipated, the azahomostatine scissile bond surrogate binds as a planar constellation consisting of seven atoms (CM, N1, CB, C, O, N, CA), all of which are less than 0.15 Å out of their least squares plane (Figure 6). A slight propeller twist of the plane around the nitrogen N1–carbonyl carbon bond is consistent with the direction of the two hydrogen bonds between the inhibitor main chain and the enzyme, O P_1' to N of Gly-76 and N P_2' to O of Gly-34. It is interesting how well this large plane is accommodated by the enzyme—both hydrogen bonds to the plane are conserved and no large deviations in volumes that are occupied by the inhibitor and enzyme side chains are observed between this and, for example, H261–endothiapepsin complex (Figure 7). Nevertheless, the twist of the plane and the distorted geometry of the two hydrogen bonds indicate that a more flexible inhibitor with a carbon atom instead of the nitrogen at P_1' would bind better. This is indeed the case—the carbon analogue CP-71,362 is roughly three times more potent (Table III). This corresponds to ~3 kJ/mol difference in the standard free energy change of the binding reactions, a distinction accounted for by the small improvement in the geometry of the two hydrogen bonds from the plane to the enzyme. Alternatively, the difference in the binding potency may be attributed to the change in an orientation of the isoleucine side chain when the planar urea nitrogen atom is substituted for the tetrahedral carbon atom (Figure 7). It must be noted that the larger negative entropy change due to the rigidification of the more flexible carbon analogue, as compared to the nitrogen analogue, is neglected in this argument. Additionally, a possible difference in solvation effects is not taken into account.

P_2 His bifurcation

$2|F_o| - |F_c|$ and $|F_o| - |F_c|$ maps obtained during refinement of the two models with only one of the two different P_2 His side chain orientations indicated that both positions are occupied. The rigorous coupled group occupancy refinement, with the model occupying both positions simultaneously, confirmed this expectation. The final occupancies are 0.43 and 0.57 for P_{2N} His and P_{2C} His, respectively.

Table IV. Differences in the positions of side chains constituting enzyme pockets[a]

Pocket	Side chains that move on inhibitor binding
S_4	**Phe-275** (3.5 Å)
S_3-S_1	**Asp-114** (1.7 Å), Glu-113 (3 Å), **Ser-110** (2.8 Å)
S_2	**Ile-297** (2.5 Å)
S_1	**Asp-77** (2 Å), Ser-79 (1.3 Å)
S_1'	Ile-213 (1 Å)
S_2'	Leu-128 (1 Å), Thr-130 (2.5 Å)
S_3'	Ser-74 (1.5 Å), **Gln-187** (2 Å), **Ile-299** (3 Å)

[a]The positions of equivalent side chains of endothiapepsin with and without the inhibitor were compared after subtraction of the rigid body movement accounting for the shifts in the main chain. Values in parentheses are approximate average distances between the equivalent side chain atoms, showing the magnitude of displacement, rotation or both. It may be noted that some side chains contribute to two enzyme pockets (Figure 4). Bold print indicates the residues that have the average side chain isotropic temperature factor greater than 20.0 Å^2.

The average isotropic temperature factors (B_{iso}) for the side chain atoms are 22.1 Å^2 for P_{2N} and 26.2 Å^2 for P_{2C}. These values are significantly lower than the average B_{iso} of 46.3 Å^2 for a model with P_{2N} His only and 36.5 Å^2 for a model with P_{2C} His only. The observed bifurcation may be attributed to either dynamic or static disorder. The S_2 pocket is large and shallow, extending to the S_1' pocket; consequently, promiscuity in inhibitor side chain binding is possible (Foundling *et al.*, 1987). Indeed, the two P_2 His orientations are interconvertible within the complex without any serious clash with enzyme atoms. Both P_2 His orientations of CP-69,799 are explored by other endothiapepsin inhibitors as well, except that none of them showed the bifurcation. Accordingly, a side chain able to fill the S_2 pocket in a manner of bifurcated histidine side chains might be a better inhibitor. It is not clear why the bifurcation is observed only with CP-69,799.

P_3-P_1 side chains orientation

CP-69,799 binds with an uncommon orientation of the P_3 phenyl ring. The P_3 phenyl orientation is conserved in the other five refined endothiapepsin complexes that have Phe at the P_3 position (H142, H77, H261, L-363,564 and H189). Yet, in CP-69,799 the P_3 phenyl ring is rotated around $C_\beta-C_\gamma$ bond for ~55° out of the plane defined by the conserved phenyl rings (Figure 7). The CP-69,799 phenyl rotamer is clearly energetically less favourable. The corresponding decrease in binding energy is estimated to be a few kJ/mol (Janin *et al.*, 1978), equivalent to ~4-fold decrease in K_i. The relative rotation can be rationalized in

terms of van der Waals contacts between the P_3 phenyl and the uniquely large cyclohexyl ring at the P_1 position (Figure 7). In addition to this difference between CP-69,799 and other inhibitors, the comparison between CP-69,799 and H261 (Figure 7) shows an accompanying change in orientation of the Asp-114 side chain participating in the S_3 pocket. This change is the only difference between H261 and CP-69,799 endothiapepsin active site clefts, except for a very small shift of the Ile-297 side chain in the S_2 pocket which correlates with a small difference in the P_{2C} imidazole position. It may be noted that in both the CP-69,799 and H261 complex the relative orientation of at least one of the Asp-114 side chain oxygens is approximately edge on to the phenyl ring at P_3. It has been observed that this is a specially stable constellation for an oxygen atom and an aromatic ring (Thomas *et al.*, 1982).

Changes in endothiapepsin molecule

A comparison of C_α positions using a difference distance matrix (for a review see Richards and Kundrot, 1988) was made between the bound and native endothiapepsin. The comparison revealed significant changes in the relative orientation of two rigid bodies, the first one comprising residues −2 to 189 and 304−326 and the second one consisting of residues 190−303. This change is conveniently interpreted within the description of the overall structural organization that portrays endothiapepsin as a large inter-domain six stranded β-sheet, on top of which two mainly β-sheet substructures are arranged in a symmetrical manner, so that the active site cleft is formed between them and that the two essential aspartates come close to each other. The top substructure of the carboxyl terminal domain is comprised of the residues 190−303 and this rotates as a rigid group by 4.1° around and moves for 0.3 Å along the screw axis, passing approximately through the C_α atoms of residues 22 and 213, and also through the active site aspartates (Figure 8). Consequently, the shape of the binding cleft is modified significantly—distances between some residues participating in formation of the cleft, change as much as 2 Å.

This rigid body movement in the endothiapepsin molecule may correspond to the conformational changes in aspartic proteinases that were suggested on the basis of the change in k_{cat}/K_m with the filling of the S_3 and S_2' pockets (Fruton, 1976; Hofmann *et al.*, 1988). The rigid body movement and its potential relevance for the mechanism of aspartic proteinases will be described in more detail elsewhere (Šali *et al.*, in preparation).

Once the differences due to rigid body movement are subtracted, no significant distortions occur upon inhibitor binding in the main chains of the two endothiapepsin forms—this includes the 'flap' region. There still remain, however, some changes in the orientation of the side chains participating in the enzyme binding pockets (Table IV). The largest change is the 3.5 Å shift of the Phe-275 ring towards the Boc group at the P_4 position, a shift resulting from the g^+ to t rotation around χ_1 of Phe-275. This rotation increases the shielding of the lipophilic N-terminal Boc group from the aqueous solvent. The significance of other smaller changes is obscured by the high isotropic temperature factors and surface position of the side chains involved (Table IV).

In the native endothiapepsin, all ten non-hydrogen side chain atoms of the two essential aspartates lie within 0.11 Å from the least squares plane defined by these atoms. The planar arrangement is slightly distorted in the CP-69,799 complex where the deviations from the plane are as large as 0.49 Å. These movements may be rationalized by the improvement in the geometry of the hydrogen bonds between P_1 OH and side chain oxygens of the aspartates 32 and 215.

The direct comparison of the isotropic temperature factors for the native endothiapepsin and its inhibitor complex was justified by the roughly equal magnitude of the lowest B_{iso} values from the two sets (Frauenfelder and Petsko, 1980). The most pronounced difference is the decrease in isotropic temperature factors for the 'flap' residues in the complex, as observed previously (Cooper *et al.*, 1987b; Suguna *et al.*, 1987b). The average B_{iso} for the atoms of the 'flap' residues 71 to 82 is 34.4 and 12.1 $Å^2$ for the free and complexed endothiapepsin, respectively (30.5 and 11.0 $Å^2$ for main chain atoms only). It is very likely that the 'flap' mobility upon inhibitor binding is reduced because of extensive hydrogen bonding and van der Waals contacts between the 'flap' and the inhibitor.

All other major differences in temperature factors involve decreases in loop regions, except for one case. This is the helix region (residues 108−115) which has average B_{iso}s of 37.2 and 15.7 $Å^2$ in the free and complexed endothiapepsin, respectively (16.0 and 8.6 $Å^2$ for main chain atoms only). This is a decrease comparable to the reduction in the 'flap' region. Since the helix is not in close contact with any of the crystallographically related molecules, the decrease in its mobility is probably also related to the inhibitor binding. However, the interactions between the inhibitor P_3 Phe and P_1 cyclohexyl side chains and the helix are not as intimate as the hydrogen bonds and van der Waals contacts between the inhibitor and the 'flap'. Consequently, other effects, for example displacement of water molecules from the enzyme active site cleft, may play a role in the decrease of the helix temperature mobility.

Comparison of endothiapepsin complexes

Comparison of nine endothiapepsin complexes (H142, H261, H256, H189, H77, L-363,564, ACRIP, BW624 and CP-69,799) reveals several common features (Blundell *et al.*, 1987; Foundling *et al.*, 1987; Cooper *et al.*, in preparation). The inhibitors bind in the active site cleft with the scissile bond surrogate positioned between the two catalytic aspartates of the enzyme. The solvent molecule located between the aspartates in the native enzyme is displaced. Inhibitor main chain conformation is conserved from the P_3 to P_2' positions. Also, the volumes occupied by P_3, P_1, P_1' and P_2' side chains are conserved. Interactions between the enzyme and inhibitor include hydrogen bonds, van der Waals contacts and ionic interactions. Seven hydrogen bonds involving inhibitor main chain are highly conserved (inhibitor atoms participating are N and O of P_2, N of P_1, O of P_1', N of P_2' and N of P_3'), whereas inhibitor side chain hydrogen bonds and hydrogen bonds to water molecules vary considerably. Pockets S_2, S_1, S_1' and S_2' are predominantly hydrophobic. Interactions at P_5, P_4, P_3' and P_3 include substantial polar character. Differences between inhibitor binding modes include bifurcated side chain orientation at P_2, deviations in the inhibitor main chain hydrogen bonding pattern to 'flap' residues Asp-77 and Gly-76, and most interestingly, different orientations of the two domains of enzyme structure (A.Šali, J.B.Cooper, B.Veerapandian and

T.L.Blundell, in preparation). Another variation is the alignment of main chains at the scissile bond surrogate. The alignments correlate with the inhibitor type: statine with five instead of three main chain atoms occupies both the S_1 and S_1' pockets, while the reduced bond inhibitors introduce a frameshift of one atom relative to the hydroxyl group of hydroxyethylene inhibitors by placing the nitrogen atom of P_1' between the two aspartates, close to the position otherwise occupied by the P_1 hydroxyl in both hydroxyethylene and statine inhibitors (Blundell *et al.*, 1987).

Conclusions

We have described the binding of the azahomostatine oligopeptide inhibitor into the endothiapepsin active site cleft. The interactions between the inhibitor, enzyme and water molecules, including hydrogen bonds and van der Waals contacts, were discussed. Changes in the enzyme structure, including differences in the position of main chain and side chains, as well as decreases in the thermal mobility, resulting from the inhibitor binding were described and sometimes rationalized. The results of this study were used to suggest possible modifications of the inhibitor structure to improve the inhibitory potency. Additionally, the relatively large domain movement observed in endothiapepsin provides a structural rationalization for the enzyme conformational changes in the action of aspartic proteinases that were indicated by several kinetic experiments.

Materials and methods

Co-crystals of endothiapepsin and CP-69,799 were grown by modification of the method by Moews and Bunn (1970). A 10-fold molar excess of the inhibitor was slowly dissolved into a 2 mg/ml solution of enzyme in 0.1 M acetate buffer at pH 4.5. The resulting precipitate was removed by centrifuging at 10 000 *g* for 30 min. Supernatant was then saturated to 55% with ammonium sulphate. Finally, a few drops of acetone were added to dissolve the precipitate caused by ammonium sulphate addition. Crystals appeared in a few weeks time.

The complex crystallized with a unit cell of $a = 42.9$ Å, $b = 75.8$ Å, $c = 42.9$ Å, $\beta = 96.9°$ in the $P2_1$ space group. Reflections were measured for three crystals to 1.80 Å resolution using Enraf–Nonius CAD4F diffractometers. Radiation damage, absorption, Lorentz and polarization corrections were applied to the total of 26 706 reflections (20.0–1.8 Å range). These were merged to give 21 985 unique reflections (corresponding to ~89% of all reflections in a 20.0–1.8 Å shell) with a merging R factor of 0.05. The observed structure factor amplitudes, $2|F_o|$, were scaled to the structure factors, $|F_c|$, computed for the endothiapepsin molecule in the appropriate unit cell, as determined previously by molecular replacement (Cooper *et al.*, in preparation). A difference electron density map calculated with coefficients $|F_o| - |F_c|$ was displayed on an Evans and Sutherland PS300 graphics system using program FRODO (Jones, 1978). A model of CP-69,799 inhibitor was then built into the difference electron density. No water molecules were added at this stage. The resulting model for the complex was subjected to stereochemically restrained least squares refinement using program RESTRAIN (Haneef *et al.*, 1985). No configurational restraints were imposed on the main chain nitrogen atom of the scissile bond surrogate. Three cycles of rigid body refinement were followed by atomic coordinate and isotropic temperature factors refinement. The electron density maps calculated with weighted $2|F_o| - |F_c|$ and $|F_o| - |F_c|$ coefficients (Read, 1986) were inspected and the model rebuilt on the graphics terminal several times during the refinement. In the later stages, water molecules were gradually added to the model, to give a total of 246 water molecules. At the end, two alternative positions for P_2 His were examined using the coupled group occupancy option of the program RESTRAIN. The final R factor $[R = \Sigma||F_o| - |F_c||/\Sigma|F_o|]$ was 0.16 for reflections in the 20–1.8 Å range ($|F_o| > 2\sigma\ |F_o|$), 20 434 reflections). The r.m.s. deviations from ideal bond distances, angle distances and peptide bond planarity are 0.012, 0.056 and 0.003 Å, respectively. The comparison of the inhibitor and enzyme isotropic temperature factors indicated that the inhibitor is present in unit occupancy. This was confirmed by the refinement of the occupancy, which gave a figure of 93.1% for the inhibitor.

The least squares fitting programs XS1 and XS2, written by A.Šali applying the method of McLachlan (1982), were used for pairwise superposition of molecules. The drawing program ARPLOT by Dr A.Lesk was used to plot the structures.

Acknowledgements

We are grateful to Dr Glenn C.Andrews (Pfizer) for synthesizing the endothiapepsin substrate and to Mrs Irene M.Purcell (Pfizer) for measuring the inhibition constants. This research was supported by Pfizer and UK SERC. A.Š. is funded by an ORS Award, Research Council of Slovenia and J.Stefan Institute, Ljubljana.

References

Akahane,K., Umeyama,H., Nakagawa,S., Moriguchi,I, Hirose,S., Iizuka,K. and Murakami,K. (1985) *Hypertension (Dallas)*, **7**, 3–12.

Andreeva,N.S, Zdanov,A.S., Gutschina,A.E. and Fedorov,A.A. (1984) *J. Biol. Chem.*, **259**, 11353–11365.

Blundell,T.L., Sibanda,B.L. and Pearl,L.H. (1983) *Nature*, **304**, 273–275.

Blundell,T.L., Jenkins,J., Pearl,L. and Sewell,T. (1985) In Kostka,V. (ed.), *Aspartic Proteinases and Their Inhibitors*. Walter de Gruyter, Berlin, pp. 151–116.

Blundell,T.L., Cooper,J. and Foundling,S.I. (1987) *Biochemistry*, **26**, 5585–5590.

Bott,R., Subramanian,E. and Davies,D. (1982) *Biochemistry*, **21**, 6956–6962.

Bott,R. and Davies,D.R. (1983) In Hruby,V.J. and Rich,D.H. (eds), *Proceedings of the 8th American Peptide Symposium*, Pierce Chemical, Rockford, IL, pp. 531–540.

Carlson,W., Karplus,M. and Haber,E. (1985) *Hypertension (Dallas)*, **7**, 13–26.

Chen,K.C.S. and Tang,J. (1972) *J. Biol. Chem.*, **247**, 2566–2574.

Chothia,C. (1974) *Nature*, **248**, 338–339.

Cooper,J.B., Foundling,S.I., Watson,F.E., Sibanda,B.L. and Blundell,T.L. (1987a) *Biochem. Soc. Trans.*, **15**, 751–754.

Cooper,J., Foundling,S.I., Hemmings,A., Blundell,T., Jones,D.M., Hallett,A. and Szelke,M. (1987b) *Eur. J. Biochem.*, **169**, 215–221.

Cooper,J., Foundling,S.I., Blundell,T.L., Arrowsmith,R.J., Harris,C.J. and Champness,J.N. (1988) In Leeming,P.R. (ed.), *Topics in Medicinal Chemistry, Roy. Soc. Chem. Special Publication*, **65**, pp. 308–313.

Fersht,A.R., Leatherbarrow,R.J. and Wells,T.N.C. (1986) *Phil. Trans. R. Soc. Lond.*, **A317**, 305–320.

Foundling,S.I., Cooper,J., Watson,F.E., Cleasby,A., Pearl,L.H., Sibanda,B.L., Hemmings,A., Wood,S.P., Blundell,T.L., Valler,T.L., Norey,K.J., Boger,J., Dunn,B.M., Leckie,B.J., Jones,D.M., Atrash,B., Hallett,A. and Szelke,M. (1987) *Nature*, **327**, 349–352.

Frauenfelder,H. and Petsko,G.A. (1980) *Biophys. J.*, **32**, 465–483.

Fruton,J.S. (1976) Adv. Enzymol., **46**, 1–36.

Haber,E. (1984) *J. Hypertens.*, **2**, 223–230.

Haber,E. and Burton,J. (1979) *FASEB Fedn. Proc.*, **38**, 2768–2773.

Hallett,A., Jones,D.M., Atrash,B., Szelke,M., Leckie,B., Beattle,S., Dunn,B.M., Valler,M.J., Rolph,C.E., Kay,J., Foundling,S.I., Wood,S., Pearl,L.H., Watson,F.E. and Blundell,T.L. (1985) In Kostka,V. (ed.), *Aspartic Proteinases and Their Inhibitors*. Walter de Gruyter, Berlin, pp. 467–478.

Haneef,I., Moss,D.S., Stanford,M.J. and Borkakoti,N. (1985) *Acta Crystallogr.*, **A41**, 426–433.

Hartsuck,J.A and Tang,J. (1972) *J. Biol. Chem.*, **247**, 2575–2580.

Hemmings,A.M., Foundling,S.I., Sibanda,B.L., Wood,S.P., Pearl,L.H. and Blundell,T.L. (1985) *Biochem. Soc. Trans.*, **13**, 1036–1041.

Hofbauer,K.G. and Wood,J.M. (1985) *Trends Pharmacol. Sci.*, **6**, 173–177.

Hofmann,T., Allen,B., Bendiner,M., Blum,M. and Cuningham,A. (1988) *Biochemistry*, **27**, 1140–1146.

James,M.N.G. and Sielecki,A. (1983) *J. Mol. Biol.*, **163**, 299–361.

James,M.N.G. and Sielecki,A. (1985) *Biochemistry*, **24**, 3701–3713.

James,M.N.G. and Sielecki,A. (1986) *Nature*, **319**, 33–38.

James,M.N.G., Sielecki,A.,R., Salituro,F., Rich,D.H. and Hofmann,T. (1982) *Proc. Natl. Acad. Sci. USA*, **79**, 6137–6142.

Janin,J., Woodak,S., Levitt,M. and Maigret,B. (1978) *J. Mol. Biol.*, **125**, 357–380.

Jones,T.A. (1978) *J. Appl. Crystallogr.*, **11**, 268–272.

McLachlan,A.D. (1982) *Acta Crystallogr.*, **A38**, 871–873.

Moews,P. and Bunn,C.W. (1970) *J. Mol. Biol.*, **54**, 395–397.

Ondetti,M.A. and Cushman,D.W. (1980) *Annu. Rev. Biochem.*, **51**, 283–308.
Pearl,L.H. and Blundell,T.L. (1984) *FEBS Lett.*, **174**, 96–101.
Ponder,J.W. and Richards,F.M. (1987) *J. Mol. Biol.*, **193**, 775–791.
Read,R.J. (1986) *Acta Crystallogr.*, **A42**, 140–149.
Richards,F.M .and Kundrot,C.E. (1988) *Proteins*, **3**, 71–84.
Richmond,T.J. and Richards,F.M. (1978) *J. Mol. Biol.*, **119**, 537–555.
Sibanda,B.L., Blundell,T.L., Hobart,P.M., Fogliano,M., Bindra,J.S., Dominiy,B.W. and Chirgwin,J.M. (1984) *FEBS Lett.*, **174**, 102–111.
Sielecki,A.R., Hayakawa,K., Fujinaga,M., Murphy,M.E.P., Fraser,M., Muir,A.K., Carilli,C.T., Lewicki,J.A., Baxter,J.D. and James,M.N.G. (1989) *Science*, **243**, 1346–1351.
Shipman,L.L. and Christoffersen,R.E. (1972) *J. Am. Chem. Soc.*, **95**, 1408–1416.
Suguna,K., Bott,R.R., Padlan,E.A., Subramanian,E., Sheriff,S., Cohen,G.E. and Davies,D.R. (1987a) *J. Mol. Biol.*, **196**, 877–900.
Suguna,K., Padlan,E.A., Smith,C.W., Carlson,W.D. and Davies,D. (1987b) *Proc. Natl. Acad. Sci. USA*, **84**, 7009–7013.
Szelke,M., Leckie,B.J., Hallett,A., Jones,D.M., Suerias-Diaz,J., Atrash,B. and Lever,A.F. (1982) *Nature*, **299**, 555–557.
Tang,J., James,M.N.G., Hsu,I.N., Jenkins,J.A. and Blundell,T.L. (1978) *Nature*, **217**, 618–621.
Thomas,K.A., Smith,G.M., Thomas,T.B. and Feldmann,R.J. (1982) *Proc. Natl. Acad. Sci. USA*, **79**, 4843–4847.
Umezawa,H., Aoyagi,T., Morishima,H., Matzusaku,M., Hamada,H. and Takeuchi,T. (1970) *J. Antibiot.*, **23**, 259–262.

Received March 3, 1989